PBT plasticity loss induced by oxidative and hydrolysis ageing

C. Loyer[a,b], G. Régnier[a], V. Duval[b], Y. Ould[b], E. Richaud[a,*]

[a] Laboratoire PIMM, Arts et Metiers Institute of Technology, CNRS, Cnam, HESAM University, 151 boulevard de l'Hopital, 75013 Paris France
[b] APTIV, Z.I des Longs Réages, 28230 Epernon France

A B S T R A C T

This paper reports the study of embrittlement of PBT submitted either to thermal or hydrolytic ageing. All changes were followed up by tensile tests, rheometry in molten state and gel permeation chromatography for molar mass changes, SAXS and DSC experiments for crystallinity changes. Both kind of ageing were shown to induce predominant chain scissions with moderate crystallinity increase, in great part due to annealing. The combination of all results were used to establish a M_w - χ_c embrittlement window helping for a determination of an end of life criterion.

Keywords:
Polybutylene terephthalate
Embrittlement
Crystallinity
Molar mass
Hydrolysis
Thermal ageing

1. Introduction

Brought to market by Celanese in the late 1960s, poly(butylene terephthalate) (PBT) is a thermoplastic polyester with a good balance between dielectric properties, mechanical strength and dimensional stability [1]. The easy processing and the rapid crystallization [2,3] makes it ideal to be processed by injection moulding. Its applications cover several fields from design insulator parts, door lockers to connectors for automotive or medical applications [4,5]. One major disadvantage is its instability regarding hydrolysis and high temperature causing its very narrow processing window (typically 250–260 °C).

In the technical literature, one can find some examples of unexpected PBT brittleness [6] where the skin-core morphology induced by injection molding is reported to be a potential failure, since this latter is well known to impact polymer properties [7–10]. The influence of morphology, especially spherulites size, on resistance and toughness has mainly been studied on PP [11–13]. It was shown that these properties are enhanced by increasing the spherulites radius but decrease above a determined value: for example a radius of 46 μm leads to a ductile behaviour whereas a radius about 126 μm leads to brittle fracture [12]. For PP, Huan et al. [13] observed that a 80 µm spherulites radius resulted in a decrease of 15 MPa of tensile strength. The process is also important: the same increase in radius but by an annealing under compression process leads to a rise of 20 MPa in tensile strength [13]. Hence, the mechanical properties are also driven by spherulites size, but these large spherulites are generally not observed in injection molding parts for PP parts [14] as well as for PBT parts.

Another reason is the possible degradation of PBT induced by the process. Polyesters are classified to be both hydrolytically and thermally unstable. Both degradation mechanisms might induce architectural changes in the macromolecular chains (chains scissions in particular) responsible for a loss of toughness. It is well documented that mechanical properties of semi-crystalline polymers depend on both molar mass and crystalline morphology. In the case of polypropylene for example, pioneering works by Fayolle [15,16] showed the embrittlement occurs when molar mass gets below a critical mass M'_c below which there is no more plastic deformation. Later, this end of life criterion was completed in the case of polyethylene [17,18], polyamide [19,20] and PLA [21]: it was highlighted that the embrittlement is also dependant on residual amorphous phase content, then crystallinity. Schematically, polymer gets brittle at low molar mass and/or low amorphous phase content and the ductile-brittle transition is represented by a line in L_a (or L_c, or χ_c) vs M_w or M_n diagram.

Despite its practical interest, the embrittlement of PBT was, to our best knowledge, scarcely addressed in scientific literature. The aim of the present paper is hence to define failure criteria corresponding to the "critical" macromolecular architecture in relation to the ductile-brittle transition. For that purpose, thin films of one PBT grade will be aged either in thermal or in hydrolytic ageing. The ageing will be systematically monitored by uniaxial tensile

* Corresponding author.
E-mail address: emmanuel.richaud@ensam.eu (E. Richaud).

tests, molar mass changes (rheometry, gel permeation chromatography) in order to give a fine description of PBT embrittlement.

2. Experimental

2.1. Material

The poly(butylene terephthalate) used in this study is an injection grade. It was transformed into films with a GIBITRE compression press (200 bar) at 230 °C. This temperature was chosen low enough to limit thermal degradation. Films were about 150 to 200 μm thick and initial average molar mass values M_n = 33.8 kg/mol and M_w = 74.7 kg/mol.

2.2. Ageing conditions

Films previously prepared were exposed to three ageing conditions:

- Thermal ageing at 180 °C and 210 °C under air in ventilated ovens (AP60 by System Climatic Service).
- Hydrolysis at 80 °C by immerging films in distilled water in closed jars placed in a ventilated oven (AP60 by System Climatic Service). After exposure, films were dried at 100 °C under vacuum overnight before any testing.

2.3. Characterization

2.3.1. Tensile testing

Uniaxial tensile testing was carried out at room temperature at 10 mm/min using an INSTRON 4301 machine with a 100 N cell. No extensometer was used during tests hence only the cross head displacement was recorded.

Samples were punched using a H3 hole punch with a 150–200 μm thickness (neck length L_0 = 20 mm and width = 4 mm).

2.3.2. Gel permeation chromatography

Gel Permeation chromatography (GPC) were performed by PeakExpert. PBT samples were dissolved in Hexafluoroisopropanol (HFiP) with 0.1 M potassium trifluoroacetate (KTFA) at 2.0 g/L. The injection volume was 100 μL at 40 °C. The detection was performed with a RID Waters 2414 refractometer. Three columns were used: one PSS PFG 10 μm, 1000 Å, ID 8,0 mm×100 mm as a pre-column and 2 columns PSS PFG 10 μm, 1000 Å, ID 8,0 mm×300 mm. Post treatment was done by using PSS-WinGPC Unity software. Molar masses were given as PMMA equivalent.

2.3.3. Differential scanning calorimetry

Morphological changes were followed with a Q1000 by TA instrument. Prior to any measurement, DSC apparatus was calibrated with an indium standard. About 6–8 mg of virgin or aged PBT sealed in standard aluminium pans were subjected to two cycles: a heating from 30 °C to 250 °C followed by a cooling 250 °C to 0 °C and the second heating from 0 °C to 250 °C and finally a cooling from 250 °C to 0 °C. Both cycles were performed at 10 °C/min rate.

The crystallinity ratio was measured by calculating the melting peak enthalpy and divided by 140 J/g [22] which is the enthalpy for a 100% crystalline PBT.

2.3.4. Rheometry

Rheology measurements were performed on MCR502 from Anton Paar with a 25 mm diameter plate geometry with a gap of 0.8 mm. Viscosity is related to weight average molar mass by:

$$\eta = KM_w^{3.4} \tag{1}$$

Frequency sweep tests from 100 to 0.1 rad/s at 230 °C were carried under nitrogen. The deformation was chosen at 2% to remain in the linear viscosity domain.

2.3.5. Small angle X-Ray scattering

The long period L_p was measured at room temperature with the diffractometer Genix Xenocs instrument using a copper anode Cu_α with λ = 1.54 Å coupled with the MAR3000 software. The distance sample to detector was 1205 mm, scattering vector Q was calibrated by using silver behenate standard sample. Samples were exposed to X-rays during 3 h on an active area of 1 mm. An exposition without any sample was also performed and used as blank and subtracted to samples spectra. After measurement, data were extracted with Foxtrot 3.2.7 software. All curves were then imported in Fityk free software and a PseudoVoigt peak find allowed finding the maximum of the wave vector Q for each curve. L_p is obtained as:

$$L_p = 2 \times \pi / Q \tag{2}$$

L_p was then used to obtain the amorphous length L_a using the following formula:

$$L_a = L_p - L_p \frac{\chi_c}{100} \tag{3}$$

where χ_c is the crystallinity of the sample.

3. Results

3.1. Mechanical changes

Aged samples were first characterized by tensile tests. For unaged PBT, the curve displays a plastic behaviour with an ultimate strain higher than 10% which is consistent with literature [23,24]. In the case of ageing at 210 °C, the curves of virgin and aged samples are almost similar in the elastic region whereas the main difference of samples having undergone oxidative and hydrolysis ageing is the absence of the plastic region (Fig. 1), which is usually observed after ageing [17,19,25].

Based on that observation, elongation at break was chosen to characterize embrittlement. The embrittlement criterion has been chosen as $\varepsilon_{R,C} = \varepsilon_0 /2$ [19]. The ageing time associated to this criterion will be called embrittlement time. Fig. 2 depicts the elongation at break with the exposure time to identified both $\varepsilon_{R,C}$ and the embrittlement time.

Firstly, the two curves for thermally-aged samples from Fig. 2 can be overlaid and the s-shape indicates that the same phenomenon occurs. According to Figs. 1 and 2, the embrittlement

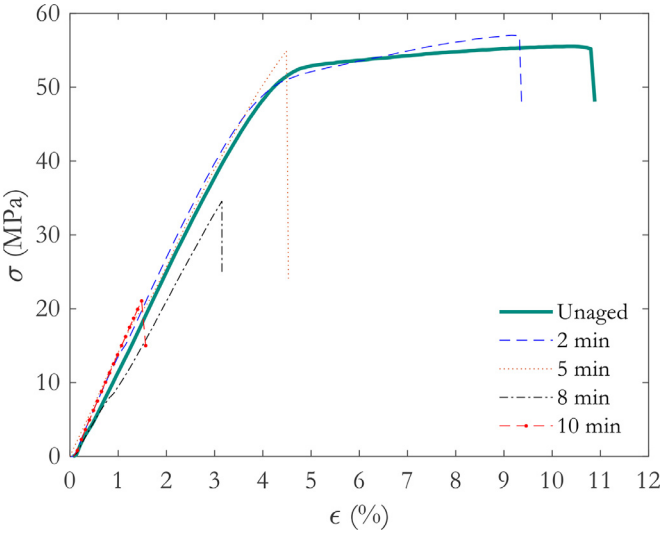

Fig. 1. Strain-stress curves for each exposure time at 210 °C. Error bars are not displayed for a clearer view.

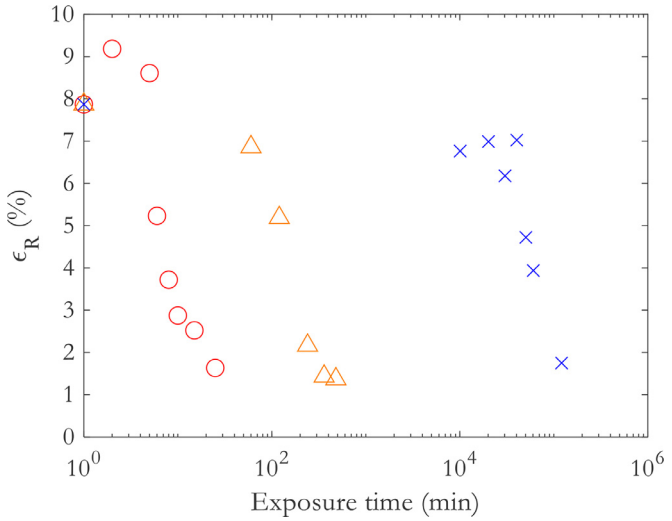

Fig. 2. Elongation at break average function of time for thermal ageing at 210 °C (○), 180 °C (△) and hydrolytic ageing at 80 °C (×). The unaged point is showed here as 10°.

time is about 8 min for ageing at 210 °C and 3 h for ageing at 180 °C and 6 weeks for a hydrolytic ageing at 80 °C.

3.2. Morphological changes

It is known that ageing has an impact on polymer semi-crystalline morphology [17]. Hence, a particular attention is paid in order to better understand the decrease in ultimate elongation. Previous studies have concluded that the decrease in elongation at break can originate from an increase in crystallinity ratio [17,19]. Nothing, to our knowledge, was reported on PBT about this possible link between ε_R and χ_c, therefore DSC measurements were performed. Fig. 3 displays thermograms for each exposure time at 210 °C under air.

For the first heating ramp (Fig. 3a), there is no change in the melting temperature for the main melting peak (located at 223 °C). However, a second melting peak appears at a temperature close to 210 °C after a very short ageing time at 210 °C (2 min) together with another one at 230 °C. The first one usually appears after annealing [26–28]. To check this hypothesis, further investigations were carried out in situ under nitrogen atmosphere in DSC. Corresponding increases in crystallinity ratio (see Fig. 3b) are relatively similar, which weights in favour of a significant annealing occurring during thermal ageing. However, the possibility of a chemicrystallization cannot be excluded at this stage, as it will be discussed later.

Both peaks contribute to an increase in melting enthalpy (Fig. 4). Crystallinity also increases from 26% for the unaged sample to 38% for the sample aged 10 min at 210 °C.

Thus, we have compared these previous results with other ageing conditions. Here is a brief summary of all observations:

- For thermal ageing at 210 °C and 180 °C: aged samples display two additional melting peaks around 210 °C peaks around 210 °C (for ageing at 210 °C) and 180 °C (for ageing at 180 °C) and 230 °C.
- For hydrolysis at 80 °C: there is one additional melting peak around 230 °C and one exothermic peak around 210 °C (see Appendix). The exothermic peak observed after hydrolysis could be associated with a partial crystallization of the amorphous phase [29], which could be consistent with the fact that chains mobility increases with exposure time due to several phenomena as explained later.

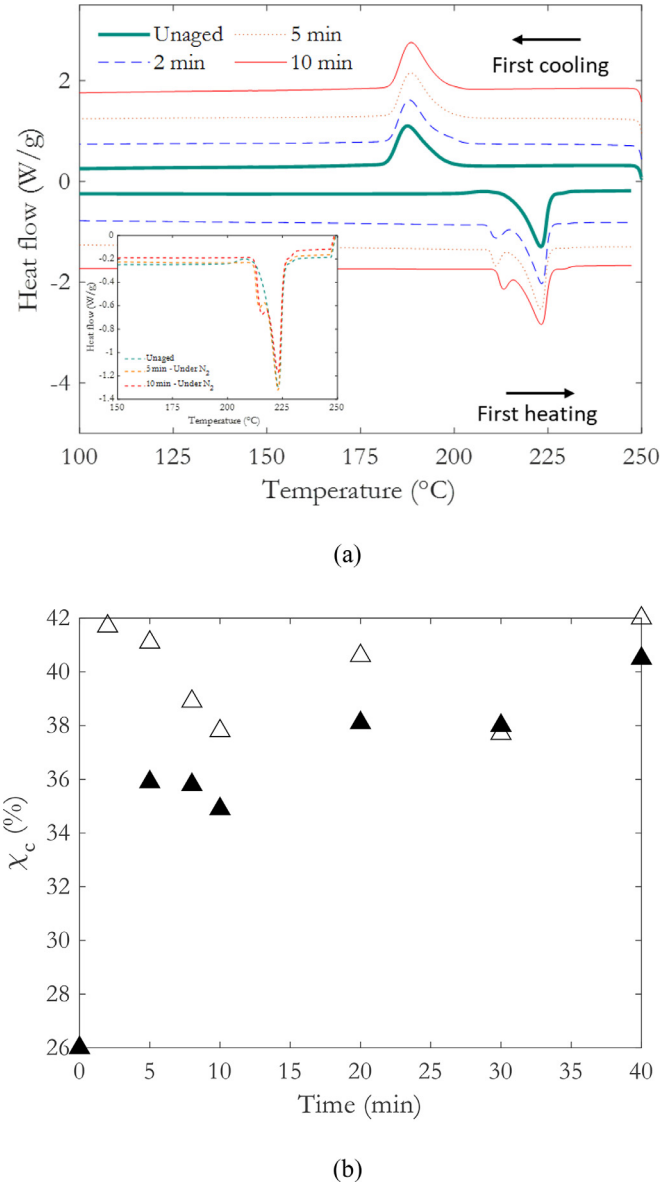

Fig. 3. Morphological evolution of PBT films thermally oxidized at 210 °C. Dashed lines are in situ N_2 exposures at 210 °C first heating (a). Comparison between thermal oxidation (△) and in situ DSC exposure (▲), both at 210 °C (b).

- Regarding all exposure conditions, the main melting peak at 223 °C does not shift towards high temperature.

According to some authors [18,19], the increase in crystalline ratio is accompanied by a thickness decrease of the amorphous layer L_a corresponding in a thickening of the crystalline part.

The decrease in L_a is well observed for each exposure condition (Fig. 5) until a minimal value around 8.5 nm at 210 °C and 80 °C and 7.5 nm at 180 °C. It also seems that the decrease is more important for the thermal oxidation at 180 °C than at 210 °C. It could go along with the earlier described phenomenon where the crystal reorganization is easier at 180 °C (corresponding approximately to the crystallization temperature) than at 210 °C which is closer to the melting peak onset (≈ 215 °C).

3.3. Macromolecular changes

Another parameter interesting for a better understanding of embrittlement is the average molar mass [18,19]. There are two

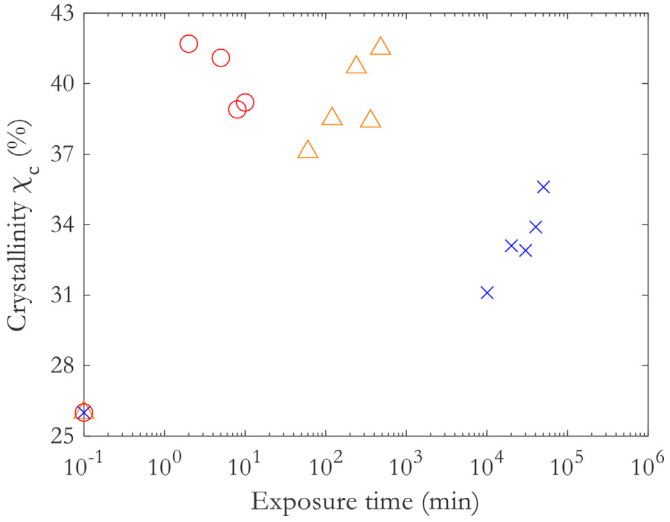

Fig. 4. Crystallinity changes for thermal ageing at 210 °C (○), 180 °C (△) and hydrolytic ageing at 80 °C (×).

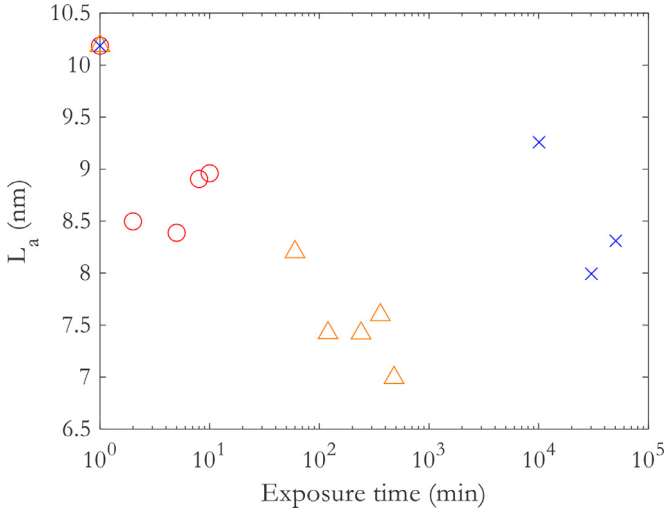

Fig. 5. Changes in thickness of the amorphous layer for thermal ageing at 210 °C (○), 180 °C (△) and hydrolytic ageing at 80 °C (×).

main experimental ways to follow macromolecular changes: GPC and viscosity, giving information about both average weight molecular mass (M_w) and the predominance of either chains scissions or crosslinking.

Some dynamic viscosity measurements are given on Fig. 6. The slight decrease of viscosity with frequency sweep is due to the rheothinning behaviour of the molten polymer. A major decrease of viscosity in the whole frequency range with exposure time can be observed. This decrease could be, with all other observations, considered as the consequence of chain scission phenomenon. Despite the small uncertainty in the measurement of $|\eta^*|$ at low frequency, M_w could be in principle determined based on the viscosity-molar mass calibration performed on unaged samples. However, rheometric experiments require the knowledge of the K factor from the initial value measured by GPC and long rheological tests at low frequency and high temperature lead to a possible degradation of the polymer.

The average weight molar masses were also measured by GPC with the additional advantage of also measuring M_z, without any further heating (contrarily to rheological measurements), hence avoiding further degradation. It allows estimating concentration

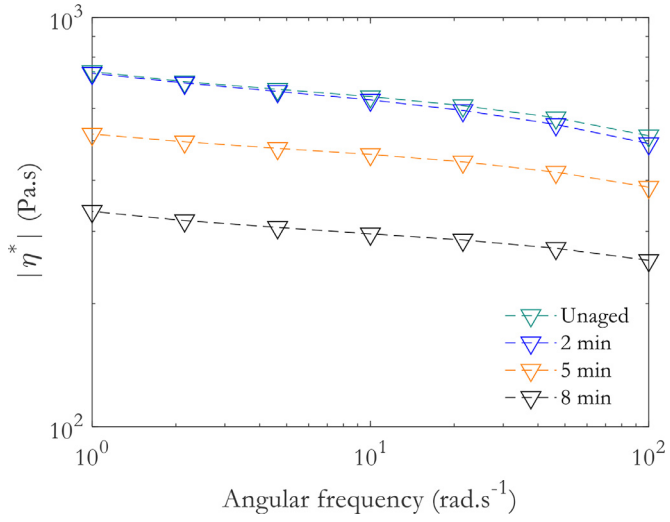

Fig. 6. Melt viscosity changes after thermal oxidation at 210 °C.

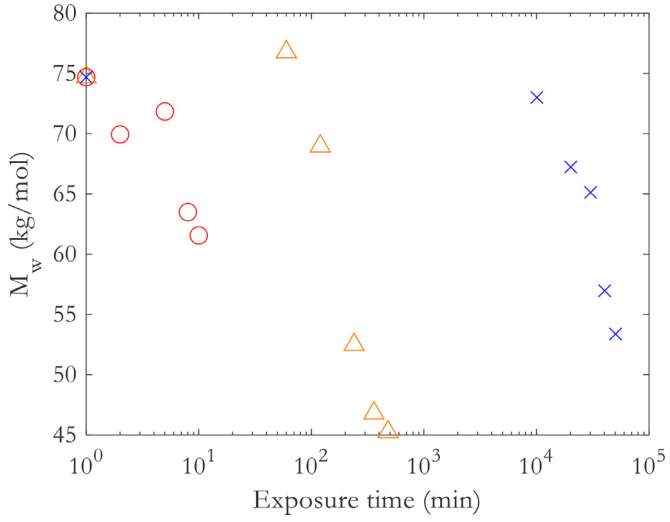

Fig. 7. Average weight molar mass changes for thermal ageing at 210 °C (○), 180 °C (△) and hydrolytic ageing at 80 °C (×). Values are given in PMMA equivalent.

in chain scissions and crosslinks as presented later in this paper. Fig. 7 gives the M_w changes (M_n and M_z are not displayed for conciseness purposes). It is noteworthy that polydispersity index does not significantly change and remains close to 2.

4. Discussion

The aim of this section is to understand the nature of architectural changes responsible for PBT embrittlement and later to illustrate commonalities and differences between PBT embrittlement and those of other semi-crystalline thermoplastics.

4.1. On the nature of macromolecular changes

The PBT degradation has been extensively studied for hydrolysis [30–33], thermolysis and thermal oxidation [34–38]. According to these references, PBT may be subject to different degradation mechanisms leading to chains scission, as depicted in Fig. 8.

PBT ageing could also lead to crosslinking through the coupling of radicals held by aromatic ring [35,39,40] (Fig. 8a). Nait-Ali et [41] have hypothesized a possible crosslinking from the coupling between aliphatic radicals (Fig. 9) which would be favored in PBT compared to PET since the concentration in methylene is higher.

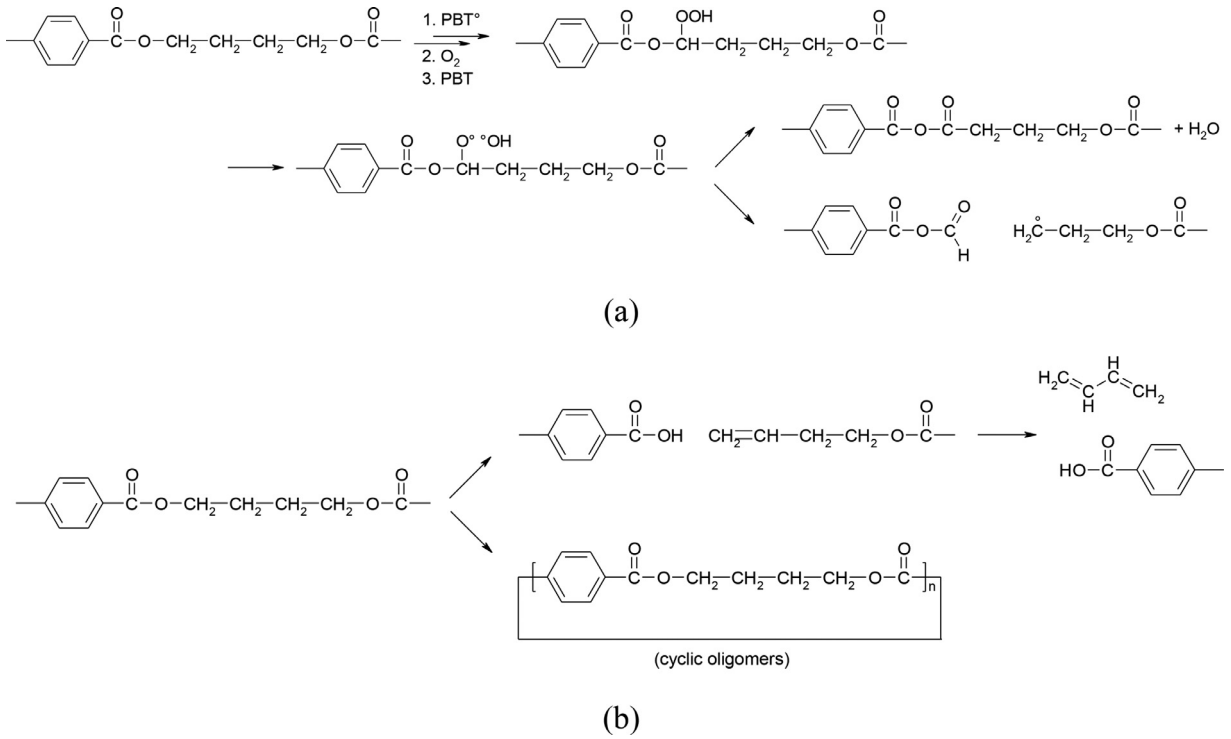

Fig. 8. Simplified thermal oxidation mechanism (a) and thermolysis of PBT (b).

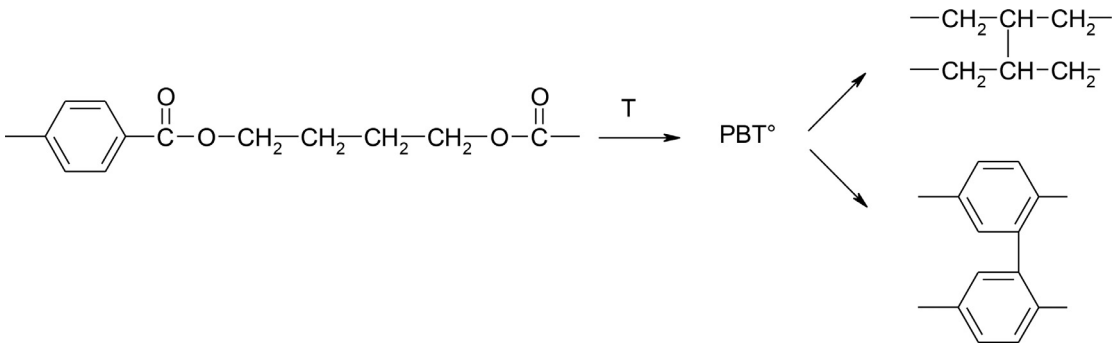

Fig. 9. Possible mechanisms of crosslinking.

Here, an analytical effort (for example mass spectrometry [35] or NMR [34]) would help to better understand the nature of the chemical changes but this goes out of the scope of the present paper aimed at understanding the consequences of ageing on mechanical properties. Despite the exact nature of the crosslinking process in PBT remains unclear, its contribution can be compared with chain scission process using the Saito's equations [42]:

$$\frac{1}{M_n} - \frac{1}{M_{n0}} = s - x \tag{4}$$

$$\frac{1}{M_w} - \frac{1}{M_{w0}} = \frac{s}{2} - 2x \tag{5}$$

With M_w average weight molar mass, M_n average number molar mass, s chain scissions and x crosslinking. Estimated s and x values are given in Fig. 10. It seems that crosslinking is clearly negligible compared to chains scissions.

It has been shown in the previous section that both M_w and ε_R decrease with exposure time. Then, it is possible to establish a link between these two quantities (Fig. 11).

It seems that a molar mass about 57–65 kg/mol would separate domains of ductile and brittle behaviour, which could be a possible

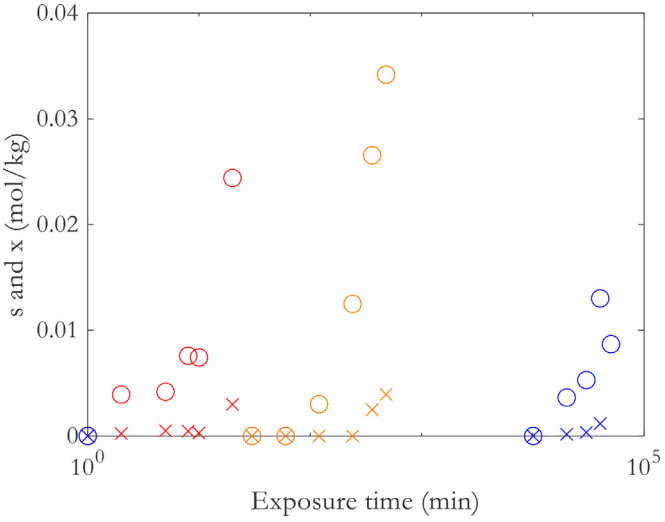

Fig. 10. Chain scission (○) and crosslinking (×) concentrations after an ageing at 210 °C (red), 180 °C (orange) and hydrolysis at 80 °C (blue).

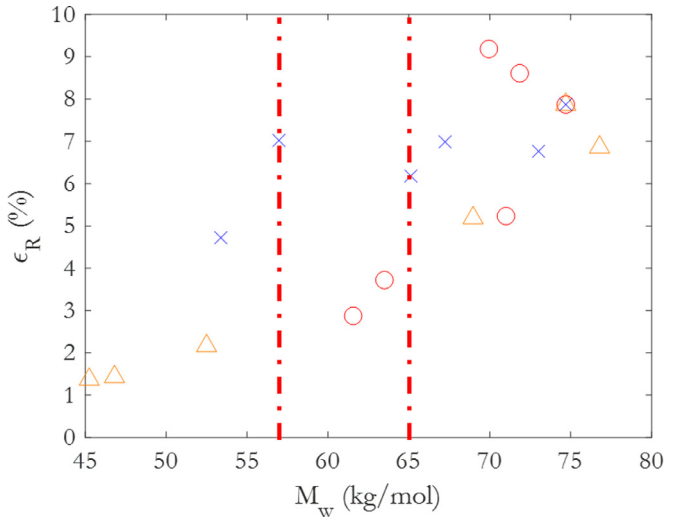

Fig. 11. Establishment of embrittlement criterion after thermal oxidation at 210 °C (○) and 180 °C (△) and hydrolytic ageing at 80 °C (×). Dashed lines represent the embrittlement frontier (respectively for 210 °C thermal ageing and hydrolytic ageing).

Table 1
Comparison between PBT and other semi-crystalline thermoplastics.

	PP	PE	POM	PET	PA11	PBT	PLA
M_e (kg/mol)	3.5	1.4	2.5	1.45–1.63	2.0	1.6	8
M'_{wc} (kg/mol)	200	70	70	22–33	20	57–65	80
M'_{wc}/M_e	57	50	28	≈10–20	10	36–41	10
Reference	[18]	[18]	[18]	[43,45,46]	[19]	[44]	[21]

failure criterion. This value can be compared with the molar mass between entanglements M_e (Table 1):

At first, M_{wc} is much higher than M_e in PBT consistently with existing literature dealing with embrittlement of semi crystalline polymers (let us recall than in amorphous polymers, M'_c/M_e is rather close to 5). Interestingly, the ratio M'_c/M_e for PBT is higher than for PET having a T_g about 20 °C higher. Last, from a practical point of view, high fluidity PBT grades used for injection purpose display generally an initial molar just above the critical molar mass value M'_c. In other words, an occurrence of a few number of chain scissions induced by the manufacturing process could lead to a strong drop in mechanical properties.

4.2. On the nature of crystalline changes during ageing

Based on the above tests results, it could be concluded that PBT undergoes annealing during its degradation process since changes in crystallinity in thermally aged PBT are relatively similar under nitrogen and under oxygen (Fig. 3b). However, the changes due to annealing are expected to occur in the earlier ageing stages whereas an increase in crystallinity seems also to be observed at later stages. Since chain scissions increase macromolecular mobility, a subsequent increase in crystallinity due to chemicrystallization might also occur as documented for example in PA11 [19] and PE [17]. To go further, the chemicrystallization yield was calculated from data given in Fig. 12 as follows:

$$y = \frac{1}{M_m}\frac{d\chi_c}{ds} \tag{6}$$

Its value was around 12 at 210 °C which is low compared to annealing of PE which are respectively equal to 4 [19] and 20 to 58 [17] (depending on the polydispersity index).

Relating to hydrolysis, the chemicrystallization yield seems slightly higher than for thermal ageing ($y = 21$ for hydrolysis) but

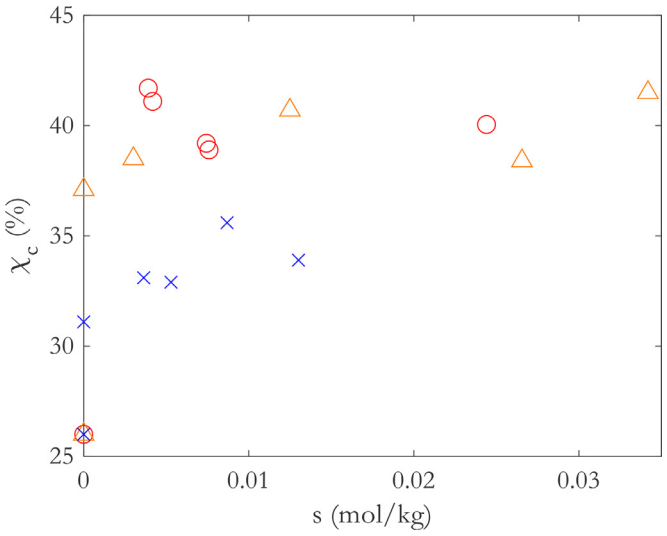

Fig. 12. Changes of crystalline versus chain scissions for thermal oxidation at 210 °C (○) and 180 °C (△) and hydrolytic ageing at 80 °C (×).

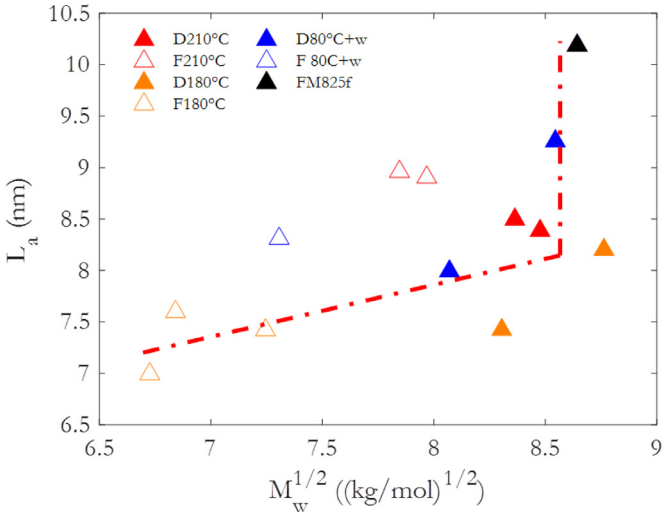

Fig. 13. Comparison of L_a for all exposition conditions. Closed triangles (▲) correspond to ductile behaviour, opened triangles (△) to brittle behaviour. The vertical line depicts the "annealing" stage and the diagonal straightline depicts the chemicrystallizaiton stage.

it remains difficult to conclude if this is an experimental incertitude or if there is a more physical mechanism linked to the presence of structural defects induced by thermal ageing or increased mobility in amorphous phase due to water plasticization.

A possible consequence of the increase in crystallinity associated with the chemicrystallization phenomenon is the thickening of the crystalline layer (Fig. 5). Under the assumption that the thickening of crystalline lamellae comes from chemicrystallization, a relation could be established between L_a and M_w [47] as investigated in Fig. 13.

Regarding Fig. 13, the decrease of L_a from 10 to around 8 nm for samples (at a constant average molar mass value) thermally aged at 180 °C and 210 °C respectively confirms that PBT mainly undergoes annealing rather than chemicrystallization in the early ageing stages. There are two identified slopes on the graph: one around 3.4 for the filled triangles and one around 1.0 for the unfilled triangles. These changes give two indications: firstly, there is a link between L_a and M_w. Secondly, there is two rates of degradation, also observed on χ_c changes. The first rate, without notice-

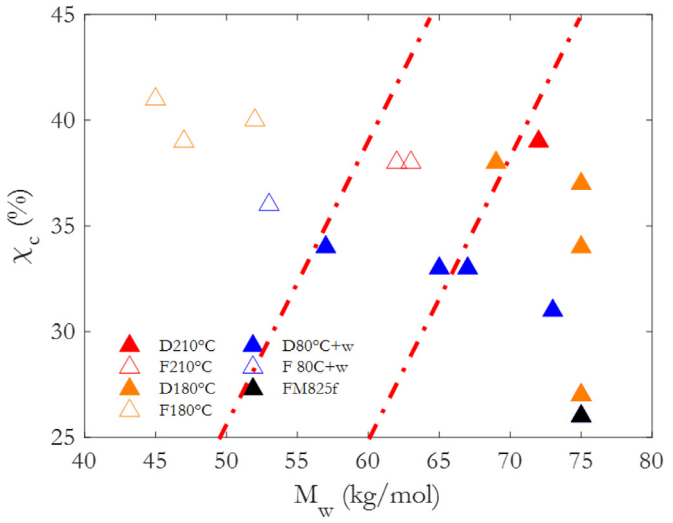

Fig. 14. Embrittlement borders according to exposure conditions. Filled triangles (▲) correspond to ductile behaviour, unfilled triangles (△) to brittle behaviour. The area between the two red dashed lines corresponds to the transition area.

able changes in M_w would be the PBT crystallization (annealing) rather than its degradation and the second rate would be related to the degradation (chemicrystallization).

It is also interesting to bring some light to the effect of observed crystallinity increase on the mechanical properties in the elastic region: in particular, Young's modulus stays almost constant (Fig. 1) which is rather unexpected. In polymers with amorphous phase in rubbery state, such as PE or PP, elastic modulus and yield stress depends heavily on the crystallinity. For instance, in PE an increase in 25% in crystalline ratio leads in an increase of 900 MPa for Young's Modulus and 8 MPa for yield stress [48]. PP displays the same trend: an increase in 5% in crystalline ratio leads to an increase of 500 MPa of Young modulus [49]. However, in polymers with their glassy amorphous phase such as PEKK, PLA or PA11 [19,50,51], the mechanical properties in the elastic domain depend less on crystallinity because the contrast of elastic modulus between crystalline phase and amorphous phase is hundred to thousand times lower [52]. At this point, it seems that PBT behaves more similarly to PA11 than to PE or PP consistently with the glassy nature of its amorphous phase.

4.3. Determination of a failure criteria

Based on the above results and observations, both crystallinity and molar mass vary during the PBT embrittlement process. We propose here an embrittlement criterion based on a combination of both properties. According to the exhaustive review by Fayolle et al. [18], the embrittlement of semi crystalline polymers may be triggered by one of the following mechanisms:

- the molar mass becomes lower than a critical value below which the amorphous phase cannot undergo plastic deformation or,
- -the molar mass goes along with a chemicrystallization process during which the thickness of intermolecular amorphous phase is reduced. This suggests a "mixed" failure criterion involving M_w and l_{ac} or M_w and χ_c.

The available data for ductile and brittle PBT samples are given in the M_w- χ_c window (Fig. 14). Dashed lines separate the domains where PBT are entirely brittle or entirely ductile. It seems well that both descriptors (macromolecular and morphological) are mandatory to predict the embrittlement of PBT. Interestingly, the straight line separating ductile and brittle domains is closer to a vertical than a horizontal line suggesting that M_w plays a predominant role over χ_c at least for thin films samples. It remains now to investigate if this conclusion is valid for other PBT grades and try to extend it to:

- bulky materials as thick dumb-bell samples, or industrial PBT connectors for example,
- other testing conditions such as impact test or tensile tests at higher elongation rates.

5. Conclusions

A PBT grade for injection purpose was thermally aged at 210 °C and 180 °C and hydrolytically aged at 80 °C to determine the evolution of the embrittlement and the associated mechanisms.

First, thermal oxidation and hydrolysis seems to cause mainly chain scission evidenced by rheometry and GPC. There was no evidence of crosslinking here but it remains to be verified for bulkier materials submitted to oxygen gradients. Those macromolecular changes are accompanied by a thickening of the crystalline phase induced by an annealing and chemicrystallization (i.e. segments liberated from chain scissions migrating to crystalline phase). These phenomena were leveragated to extract a failure criterion. Samples get brittle when molar mass is below a critical value M'_c close to 60 kg/mol i.e. almost 40 times higher than the molar mass between entanglements. Such a high value suggests that a very limited occurrence of chain scission is needed to induce a severe plasticity loss in PBT. The ratio between molar mass at embrittlement and molar mass between entanglements is in line with other semi crystalline polymers and much higher than in glassy polymers (where typically M'_c/M_e is close to 5). It means that changes in the crystalline phase are also involved in PBT embrittlement. Basing on these observations, a M_{wc}-χ_c window separating two domains corresponding to ductile and brittle behaviour was proposed for the first time. In the next steps, this will be used to investigate the embrittlement of injection molded parts for which the molten polymer viscosity must be low meaning that the initial value of molar mass is close to the critical molar mass for embrittlement.

Declaration of Competing Interest

We hereby confirm that we have no conflict of interest with the paper

CRediT authorship contribution statement

C. Loyer: Data curation, Formal analysis, Investigation, Writing - original draft, Writing - review & editing. **G. Régnier:** Conceptualization, Funding acquisition, Methodology, Project administration, Supervision, Validation, Writing - original draft. **V. Duval:** Conceptualization, Funding acquisition, Methodology, Project administration, Supervision, Validation, Writing - original draft, Writing - review & editing. **Y. Ould:** Conceptualization, Funding acquisition, Methodology, Project administration, Supervision, Validation, Writing - original draft. **E. Richaud:** Conceptualization, Funding acquisition, Methodology, Project administration, Supervision, Validation, Writing - original draft, Writing - review & editing.

Acknowledgments

The authors would like to thank the ANRT for granting this project (N°2019/1467).

The authors would also like to thank V. Michel, RX manager at PIMM laboratory for helping in SAXS measurements and data treatment.

Appendix

DSC of PBT after hydrolysis (Fig. 15).

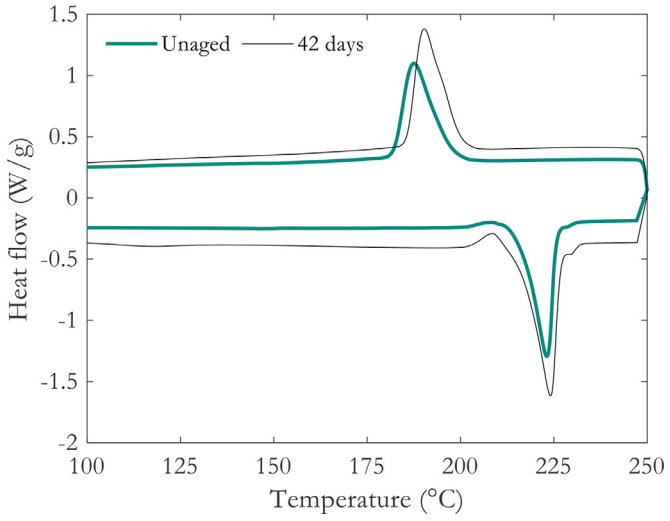

Fig. 15. First heat and cooling after hydrolysis at 80 °C.

References

[1] H.-J. Radusch, Poly(Butylene Terephthalate), in: S. Fakirov (Ed.), Handbook of Thermoplastic Polyesters, 1st ed., Wiley, 2002, pp. 389–419.

[2] S.Z.D. Cheng, R. Pan, B. Wunderlich, Thermal analysis of poly(butylene terephthalate) for heat capacity, rigid-amorphous content, and transition behavior, Die Makromolekulare Chemie 189 (10) (1988) 2443–2458, doi:10.1002/macp.1988.021891022.

[3] M. Pyda, E. Nowak-Pyda, J. Heeg, H. Huth, A.A. Minakov, M.L. Di Lorenzo, C. Schick, B. Wunderlich, Melting and crystallization of poly(butylene terephthalate) by temperature-modulated and superfast calorimetry, J. Polym. Sci. B Polym. Phys. 44 (9) (2006) 1364–1377, doi:10.1002/polb.20789.

[4] T. Johnson, The many uses of PBT plastics, Thougtco (2019) Aug. 11 https://www.thoughtco.com/what-are-pbt-plastics-820360 . accessed Mar. 31, 2020.

[5] Complete Guide on Polybutylene Terephthalate(PBT), Omnexus (2020) https://omnexus.specialchem.com/selection-guide/polybutylene-terephthalate-pbt-plastic. accessed Mar. 31.

[6] M. Völkel, C. Staller, A. Eipper, Brittle Fracture in PBT, Kunststoffe Plast. Eur. 9 (2005) 191–194.

[7] M.B. Baradi, A step towards predicting the mechanical properties of weld lines in injection-molded short fiber-reinforced thermoplastics, Ecole nationale supérieure des arts et métiers (2019).

[8] J.E. Callear, J.B. Shortall, The effect of microstructure and crystallinity on the tensile properties and fracture behaviour of injection-moulded polytetramethylene terephthalate, J. Mater. Sci. 12 (1) (1977) 141–152, doi:10.1007/BF00738479.

[9] H.-J. Ludwig, P. Eyerer, Influence of the processing conditions on morphology and deformation behavior of poly(butylene terephthalate) (PBT), Polym. Eng. Sci. 28 (3) (1988) 143–146, doi:10.1002/pen.760280304.

[10] E. Hnatkova, Z. Dvorak, Effect of the skin-core morphology on the mechanical properties of injection-moulded parts, Mater. Tehnol. 50 (2) (2016) 195–198, doi:10.17222/mit.2014.151.

[11] A. Lustiger, C.N. Marzinsky, R.R. Mueller, Spherulite boundary strengthening concept for toughening polypropylene, J. Polym. Sci. B Polym. Phys. 36 (1998) 2047–2056.

[12] J.L. Way, J.R. Atkinson, J. Nutting, The effect of spherulite size on the fracture morphology of polypropylene, J. Mater. Sci. 9 (2) (1974) 293–299, doi:10.1007/BF00550954.

[13] Q. Huan, S. Zhu, Y. Ma, J. Zhang, S. Zhang, X. Feng, K. Han, M. Yu, Markedly improving mechanical properties for isotactic polypropylene with large-size spherulites by pressure-induced flow processing, Polymer 54 (3) (2013) 1177–1183, doi:10.1016/j.polymer.2012.12.055.

[14] R. Mendoza, G. Régnier, W. Seiler, J.L. Lebrun, Spatial distribution of molecular orientation in injection molded iPP: influence of processing conditions, Polymer 44 (11) (2003) 3363–3373, doi:10.1016/S0032-3861(03)00253-2.

[15] B. Fayolle, L. Audouin, J. Verdu, Oxidation induced embrittlement in polypropylene — A tensile testing study, Polym. Degrad. Stab. 70 (3) (2000) 333–340, doi:10.1016/S0141-3910(00)00108-7.

[16] B. Fayolle, L. Audouin, J. Verdu, A critical molar mass separating the ductile and brittle regimes as revealed by thermal oxidation in polypropylene, Polymer 45 (12) (2004) 4323–4330, doi:10.1016/j.polymer.2004.03.069.

[17] A.F. Reano, A. Guinault, E. Richaud, B. Fayolle, Polyethylene loss of ductility during oxidation: effect of initial molar mass distribution, Polym. Degrad. Stab. 149 (2018) 78–84, doi:10.1016/j.polymdegradstab.2018.01.021.

[18] B. Fayolle, E. Richaud, X. Colin, J. Verdu, Review: degradation-induced embrittlement in semi-crystalline polymers having their amorphous phase in rubbery state, J. Mater. Sci. 43 (22) (Nov. 2008) 6999–7012, doi:10.1007/s10853-008-3005-3.

[19] O. Okamba-Diogo, E. Richaud, J. Verdu, F. Fernagut, J. Guilment, B. Fayolle, Investigation of polyamide 11 embrittlement during oxidative degradation, Polymer 82 (2016) 49–56, doi:10.1016/j.polymer.2015.11.025.

[20] S.J.A. Hocker, W.T. Kim, H.C. Schniepp, D.E. Kranbuehl, Polymer crystallinity and the ductile to brittle transition, Polymer 158 (2018) 72–76, doi:10.1016/j.polymer.2018.10.031.

[21] D. Rasselet, A. Ruellan, A. Guinault, G. Miquelard-Garnier, C. Sollogoub, B. Fayolle, Oxidative degradation of polylactide (PLA) and its effects on physical and mechanical properties, Eur. Polym. J. 50 (Jan. 2014) 109–116, doi:10.1016/j.eurpolymj.2013.10.011.

[22] K.-H. Illers, Heat of fusion and specific volume of poly(ethylene terephthalate) and poly(butylene terephthalate, Colloid Polymer Sci. 258 (2) (1980) 117–124, doi:10.1007/BF01498267.

[23] S. Hashemi, Fracture of polybutylene terephthalate (PBT) film, Polymer 43 (2002) 4033–4041.

[24] S. Hashemi, A. Arkhireyeva, Influence of temperature on work fracture parameters in semi-crystalline polyesters films, J. Macromol. Sci. Part B 41 (4–6) (2002) 863–880, doi:10.1081/MB-120013070.

[25] M. Arhant, M. Le Gall, P.-Y. Le Gac, P. Davies, Impact of hydrolytic degradation on mechanical properties of PET - towards an understanding of microplastics formation, Polym. Degrad. Stab. 161 (2019) 175–182, doi:10.1016/j.polymdegradstab.2019.01.021.

[26] J. Kim, M.E. Nichols, R.E. Robertson, The annealing and thermal analysis of poly(butylene terephthalate), J. Polym. Sci. B Polym. Phys. 32 (5) (1994) 887–899, doi:10.1002/polb.1994.090320512.

[27] D. Bassett, R. Olley, I. Alraheil, On crystallization phenomena in PEEK☆, Polymer 29 (10) (1988) 1745–1754, doi:10.1016/0032-3861(88)90386-2.

[28] K. Jariyavidyanont, R. Androsch, C. Schick, Crystal reorganization of poly (butylene terephthalate), Polymer 124 (2017) 274–283, doi:10.1016/j.polymer.2017.07.076.

[29] J.T. Yeh, J. Runt, Multiple melting in annealed poly(butlene terephthalate), J. Polym. Sci. B Polym. Phys. 27 (7) (1989) 1543–1550, doi:10.1002/polb.1989.090270714.

[30] A.S. Goje, Auto-Catalyzed Hydrolytic Depolymerization of Poly(Butylene Terephthalate) Waste at High Temperature, Polym. Plast. Technol. Eng. 45 (2) (2006) 171–181, doi:10.1080/03602550500374012.

[31] Z.A.M. Ishak, A. Ari, Effects of hygrothermal aging and a silane coupling agent on the tensile properties of injection molded short glass ®ber reinforced poly(butylene terephthalate) composites, Eur. Polym. J. (2001) 13.

[32] Z.A.M. Ishak, N.C. Lim, Effect of moisture absorption on the tensile properties of short glass fiber reinforced poly(butylene terephthalate), Polym. Eng. Sci. 34 (22) (1994) 1645–1655, doi:10.1002/pen.760342202.

[33] P.G. Kelleher, R.P. Wentz, D.R. Falcone, Hydrolysis of poly(butylene terephthalate), Polym. Eng. Sci. 22 (4) (1982) 260–264, doi:10.1002/pen.760220408.

[34] F. Samperi, C. Puglisi, R. Alicata, G. Montaudo, Thermal degradation of poly(butylene terephthalate) at the processing temperature, Polym. Degrad. Stab. 83 (1) (Jan. 2004) 11–17, doi:10.1016/S0141-3910(03)00167-8.

[35] S. Carroccio, P. Rizzarelli, G. Scaltro, C. Puglisi, Comparative investigation of photo- and thermal-oxidation processes in poly(butylene terephthalate), Polymer 49 (16) (2008) 3371–3381, doi:10.1016/j.polymer.2008.05.015.

[36] S.-J. Chiu, Y.-S. Wu, A comparative study on thermal and catalytic degradation of polybutylene terephthalate, J. Anal. Appl. Pyrolysis. 86 (1) (2009) 22–27, doi:10.1016/j.jaap.2009.03.003.

[37] N. Manabe, Y. Yokota, The method for analyzing anhydride formed in poly(butylene terephthalate) (PBT) during thermal and photo-degradation processes and applications for evaluation of the extent of degradation, Polym. Degrad. Stab. 69 (2) (2000) 183–190, doi:10.1016/S0141-3910(00)00059-8.

[38] G. Montaudo, C. Puglisi, F. Samperi, Primary thermal degradation mechanisms of Poly(ethylene terephthalate) and Poly(butylene terephthalate), Polym. Degrad. Stab. 42 (1) (1993) 13–28, doi:10.1016/0141-3910(93)90021-A.

[39] A. Rivaton, Photochemistry of poly(butyleneterephthalate): 2—Identification of the IR-absorbing photooxidation products, Polym. Degrad. Stab. 41 (3) (1993) 297–310, doi:10.1016/0141-3910(93)90076-U.

[40] A. Rivaton, F. Serre, J.L. Gardette, Oxidative and photooxidative degradations of PP/PBT blends, Polym. Degrad. Stab. 62 (1) (1998) 127–143, doi:10.1016/S0141-3910(97)00271-1.

[41] L.K. Nait-Ali, X. Colin, A. Bergeret, Kinetic analysis and modelling of PET macromolecular changes during its mechanical recycling by extrusion, Polym. Degrad. Stabil. 96 (2) (2011) 236–246, doi:10.1016/j.polymdegradstab.2010.11.004.

[42] O. Saito, Effects of high energy radiation on polymers II. End-linking and gel fraction.pdf, J. Phys. Soc. Jpn. 13 (12) (1958) 1451–1464.

[43] L. Gervat, Structure, Propriétés Mécaniques Et Renforcement Au Choc Du PBT, 6, Paris, 1999.

[44] CROW, 'Poly(butylene terephthalate), Polym. Propert. Datab. (2019) https://polymerdatabase.com/polymers/polybutyleneterephthalate.html.

[45] L.J. Fetters, D.J. Lohse, R.H. Colby, in: Chain Dimensions and Entanglement Spacing, Springer, New York, NY, 2007, pp. 447–454.

[46] J.M. Stearne, I.M. Ward, The tensile behaviour of polyethylene terephthalate, J. Mater. Sci. 4 (12) (1969) 1088–1096, doi:10.1007/BF00549849.

[47] J. Rault, E. Robelin-Souffaché, Long periods in slow-cooled linear and branched polyethylene: part II, J. Polym. Sci. B Polym. Phys. 27 (6) (1989) 1349–1373, doi:10.1002/polb.1989.090270612.
[48] K. Jordens, The influence of molecular weight and thermal history on the thermal, rheological, and mechanical properties of metallocene-catalyzed linear polyethylenes, Polymer 41 (19) (2000) 7175–7192, doi:10.1016/S0032-3861(00)00073-2.
[49] B. Pukánszky, I. Mudra, P. Staniek, Relation of crystalline structure and mechanical properties of nucleated polypropylene, J Vinyl Addit Technol 3 (1) (1997) 53–57, doi:10.1002/vnl.10165.
[50] T. Choupin, 'Mechanical performances of PEKK thermoplastic composites linked to their processing parameters', Thesis. ENSAM (2017). p. 143.
[51] H. Li, M.A. Huneault, Effect of nucleation and plasticization on the crystallization of poly(lactic acid), Polymer 48 (23) (2007) 6855–6866 Nov., doi:10.1016/j.polymer.2007.09.020.
[52] F. Bedoui, J. Diani, G. Regnier, W. Seiler, Micromechanical modeling of isotropic elastic behavior of semicrystalline polymers, Acta Mater. 54 (6) (2006) 1513–1523 Apr., doi:10.1016/j.actamat.2005.11.028.